

# Redistribution of electronic charges in spin-Peierls state in $(\text{TMTTF})_2\text{AsF}_6$ observed by $^{13}\text{C}$ NMR

Shigeki Fujiyama\* and Toshikazu Nakamura

*Institute for Molecular Science, Myodaiji, Okazaki 444-8585, Japan*

(Dated: May 23, 2019)

We report  $^{13}\text{C}$  NMR spectra and nuclear spin lattice relaxation rate  $1/T_1$  for a quasi-one-dimensional quarter-filled organic material  $(\text{TMTTF})_2\text{AsF}_6$ , which undergoes charge ordering ( $T_{\text{CO}} = 102$  K) and spin-Peierls phase transitions ( $T_{\text{SP}} = 12$  K). The ratio of two  $1/T_1$  for the charge accepting and donating TMTTF sites which grows from  $T_{\text{CO}}$  finally saturates in approaching  $T_{\text{SP}}$ , indicating one spin correlation function even in the charge ordered state. Below  $T_{\text{SP}}$ , however, the doubly split NMR lines from inequivalently charged molecules merge into one line, originated from the variation in *charge* densities. This shows that a rearrangement of the charge configuration occurs at  $T_{\text{SP}}$ .

PACS numbers: 71.20.Rv, 71.30.+h, 71.45.-d, 76.60.-k

## I. INTRODUCTION

There has been considerable interest in correlated electrons in low dimensional systems. There, interplay between spin, charge, and lattice degrees of freedom becomes relevant to the macroscopic physical properties, resulting in various electronic states. Recent developments on inorganic materials such as high- $T_c$  cuprates or manganites have revealed that electronic states can be highly inhomogeneous due to the complex interplay among these degrees of freedom.<sup>1,2,3</sup>

Organic charge transfer salts (CTS) also provide model systems of strongly correlated low dimensional electrons. Recent experimental and theoretical developments on the organic conductors have revealed that in some compounds the electronic charges are disproportionated (ordered), namely, inhomogeneous electronic states are realized.<sup>4</sup> Observations of anomalous dielectric relaxation, superstructures by X-ray diffraction (XRD), and shifts of Raman frequencies stemmed from the vibration of variedly charged molecules have indicated such inhomogeneous electronic states.<sup>5,6,7,8,9</sup> Although recent theoretical developments have revealed that Coulomb repulsion among the electronic charges is indispensable to the charge ordering, various orderings have been proposed such as  $2k_F$ -spin density wave (SDW),  $2k_F$ -charge density wave (CDW),  $4k_F$ -CDW, and also the varieties of their coexistences.<sup>10,11,12,13,14,15,16,17,18</sup>

It is well recognized that NMR technique has played a key role in elucidating the electronic states of organic conductors since the hyperfine field is proportional to the spin density of each nucleus. By this reason, NMR on the  $^{13}\text{C}$  labeled CTS is much more sensitive to the change of the electronic properties than that on  $^1\text{H}$  since the spin densities on the central carbons in organic CTS is richer. In fact, several NMR measurements have so far revealed the occurrence of charge ordering in organic conductors. A line splitting of the  $^{13}\text{C}$  NMR spectra in the semiconducting temperature range was first demonstrated for a powder sample of quasi-one-dimensional (Q1D)  $(\text{DI-DCNQI})_2\text{Ag}$ , that showed im-

balanced charged molecules.<sup>19</sup> For quasi-two-dimensional organic conductors, an anomalous line broadening originated from one carbon site and the corresponding differentiation in  $1/T_1$  were reported for a single crystal of  $\theta$ -(BEDT-TTF) $_2\text{RbZn}(\text{SCN})_4$ .<sup>20</sup> These two studies clearly shows the charge ordering from the microscopic point of view.

Charge ordering has also been indicated in members in the family of  $(\text{TMTCF})_2X$  ( $C = \text{Se, S}$ ), also known as the Bechgaard salts and their sulphur analogues. Their physical properties have been extensively studied so far because the materials realize various ground states by modifying chalcogens ( $C$ ) and/or anions ( $X$ ).<sup>21</sup> In addition to the chemical pressure effect which is controlled by the substitution of  $C$  or  $X$ , it is well established that physically applied pressure can easily change the electronic state of this series of materials. Their macroscopic electronic properties are summarized in a pressure ( $P$ ) vs. temperature ( $T$ ) phase diagram.<sup>22</sup> In this phase diagram the ground state varies as spin-Peierls state, antiferromagnet, SDW, and superconductivity, from low- $P$  side to high- $P$  side. The electronic properties are extensively investigated theoretically as well, based on models for quarter-filled Q1D electronic systems.<sup>23,24</sup>

The charge ordering in TMTTF CTS was first indicated for the members that have antiferromagnetic ground states. The dependence of the  $^1\text{H}$ -NMR spectra on the direction of the external magnetic field for  $(\text{TMTTF})_2\text{Br}$  and  $(\text{TMTTF})_2\text{SCN}$  suggests that nodes of spin density exist on the TMTTF molecules.<sup>25,26</sup> A theoretical proposal including intersite repulsive interaction suggests an (up-0-down-0) magnetic structure as their ground state<sup>13</sup> and a recent  $^{13}\text{C}$  NMR study by the present authors on  $(\text{TMTTF})_2\text{SCN}$  confirms the charge ordering as well as this charge (spin) configuration.<sup>27</sup>

In the  $P$ - $T$  phase diagram,  $(\text{TMTTF})_2\text{AsF}_6$  and  $(\text{TMTTF})\text{PF}_6$  are located at the low- $P$  end which indicates the narrowest bandwidth. The resistivities for both materials have their minima at about 200 K, and the ground states are known to be a spin-Peierls state.<sup>28,29</sup> The charge disproportionation in the TMTTF CTS was

clearly demonstrated for the first time in these two materials by the spectral and  $1/T_1$  studies of  $^{13}\text{C}$  NMR.<sup>30,31</sup> In Refs. 30 and 31, two distinct lines in the  $^{13}\text{C}$  NMR spectra appear to split with roughly equal intensities below about 100 K. Correspondingly, two  $1/T_1$  appear due to the existence of unequal charge densities. It is argued that  $1/T_1$  for the charge accepting and donating sites show different temperature dependences, and moreover,  $1/T_1$  for the charge rich sites becomes independent of temperature between 40 K and 80 K indicating one dimensional “magnetic” correlations among spin 1/2’s realized at the charge accepting sites. It is also found that under hydrostatic pressure, the phase transition temperature to the charge ordered state ( $T_{\text{CO}}$ ) steeply decreases against pressure, and  $T_{\text{CO}}$  vanishes at pressure as low as 0.15 GPa. It is proposed that the low temperature electronic state at ambient pressure is a coexistence of the charge ordering and the spin-Peierls state, which is fragile under pressure.

In this paper, we demonstrate results on the frequency shifts and nuclear spin lattice relaxation rate  $1/T_1$  for the  $^{13}\text{C}$  labeled  $(\text{TMTTF})_2\text{AsF}_6$  from room temperature down to 2 K. Below 102 K, the splitting of the NMR spectra and the appearance of two  $1/T_1$  with different temperature dependences evidence the appearance of inequivalent molecules with imbalanced charge densities. These are consistent with the previously reported data in Refs. 30 and 31. We have successfully measured the ratio of  $1/T_1$  of the charge accepting and donating sites down to the lowest temperature, for the first time, and pursue the development of the charge ordering. This ratio, suggesting the ratio in the charge densities to be 2:1, finally saturates in approaching  $T_{\text{SP}}$ , which reveals only one spin correlation function even in the charge ordered state. However, at  $T_{\text{SP}}$  the line splitting disappears, which we argue to be originated from the variation in charge densities. This shows a strong suppression of charge ordering or a redistribution of charge densities due to the phase transition from the charge ordered paramagnetic state to the spin-Peierls state.

## II. EXPERIMENTS

A rectangular needle-like single crystal of  $(\text{TMTTF})_2\text{AsF}_6$  in which the two central carbon sites on the TMTTF molecules are labeled with  $^{13}\text{C}$  was prepared by standard electrochemical oxidation method.

The uniform susceptibility ( $\chi$ ) of our sample linearly decreases from  $6 \times 10^{-4}$  [emu/mol] at 300 K to  $3.7 \times 10^{-4}$  [emu/mol] at 20 K. However the  $\chi$  shows a strong drop at 11 K and the electronic state undergoes to the spin-Peierls state.

The NMR measurements were performed by using a standard pulsed NMR spectrometer operated at about 87.1 MHz with the bandwidth of 300 kHz for a single crystal. The spectra were obtained by the Fourier transformation (FT) of the spin echo refocused by applying

$\pi/2$  and  $\pi$  rf-pulses with the time interval of  $20\mu\text{s}$ . The nuclear recovery data were obtained by integrating the intensities of distinct lines of the spectra in the frequency domain by saturation recovery method.  $1/T_1$  were defined by fitting them to a single exponential formula.

## III. PARAMAGNETIC STATE

### A. Angular dependence of the spectra for the present experimental setting

The previously reported Knight shift for TMTTF CTS in which central double-bonded carbon sites are substituted by  $^{13}\text{C}$  have smaller temperature dependence than those for BEDT-TTF salts, although the uniform susceptibilities for both systems have similar values at room temperatures.<sup>27,31</sup> Under such condition, it is difficult to obtain the hyperfine coupling tensor for  $^{13}\text{C}$  NMR by just plotting the Knight shift against uniform susceptibility ( $K-\chi$  plot).

Therefore, we first perform show the angular dependence of spectral frequencies under the rotation of magnetic field in the  $b$ - $c$  plane. The results for high temperature (220 K) and low temperature (5 K) are shown in Fig. 1. The expected origins for these frequency shifts are the Knight (spin) shift, the chemical shift, and the nuclear dipolar interaction.

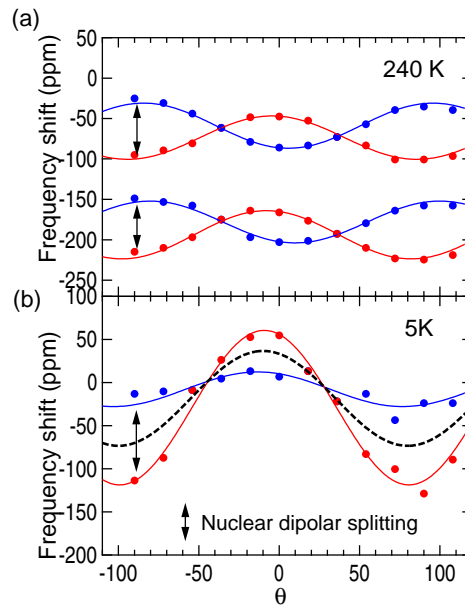


FIG. 1: Angular dependence of the peak positions of the NMR spectra rotated in the  $b$ - $c$  plane at 240 K (a) and 5 K (b).

The electronic state of  $(\text{TMTTF})_2\text{AsF}_6$  below 12 K is known to be the spin-Peierls state as mentioned above, so the Knight shift is negligible in Fig. 1 (b). Therefore, the sources for the angular dependence of the spectra at

5 K should be the anisotropy in the chemical shifts and that in the nuclear dipolar interaction. In Fig. 1 (b), the contribution from the nuclear dipolar interaction is indicated as vertical arrows, which have the same angular dependence as those in the paramagnetic state. The angular dependence of the chemical shift is therefore obtained by plotting the midpoints between the two peaks, as shown as the dashed line in Fig. 1 (b).

The small angular dependence of the mid points of the peak positions of the spectra in the paramagnetic state as shown in Fig. 1 (a) indicates that both the chemical shift and the Knight shift have nearly the same magnitudes but with opposite signs when we apply the external magnetic field perpendicular to the *a* axis.

Now let us explain this more detail in the following. The anisotropy of the chemical shift for the central carbons in the TMTTF molecule can be speculated from that for the BEDT-TTF molecule, which is well known, since the local bonds connected to the central carbons in the TMTTF and BEDT-TTF molecules are similar to each other. For BEDT-TTF it is reported as (-24, 88, -64) [ppm], where *z* axis is defined as the direction perpendicular to the plane of the BEDT-TTF molecule, *x*(*y*) axis is defined as the long (short) axis parallel to the molecular plane<sup>32</sup>. Therefore, for TMTTF also, we can consider that the most shielding axis is perpendicular to the molecular plane.<sup>33</sup>

With regard to spin contribution to the frequency shift, according to molecular orbital calculations, the dominating character of the central carbon site participating in the highest occupied molecular orbital is the  $2p_z$  orbital, where *z* is the direction perpendicular to the plane of TMTTF molecule.<sup>21</sup> When the small dipolar field from the other orbitals than  $^{13}\text{C}$   $2p_z$  is neglected, the frequency shift *K* is expected to have a uniaxial symmetry,  $K(\theta) = K_{\text{iso}} + (1 - 3 \cos^2 \theta)K_{\text{ax}}$ . Here  $\theta$  is the angle between the external field and the *z*-axis,  $K_{\text{iso}}(K_{\text{ax}})$  is the isotropic (anisotropic) part of the magnetic frequency shift, which is related to the spin susceptibility ( $\chi$ ) by  $K_{\text{iso,ax}} = F_{\text{iso,ax}}\chi/2N_A\mu_B$ ;  $N_A$  is the Avogadro's number and  $\mu_B$  is the Bohr magneton. The quantity  $F_{\text{ax}}$  is proportional to the spin density in the  $2p_z$  orbital as  $F_{\text{ax}} = \frac{2}{3}\langle r^{-3} \rangle_{2p}\mu_B\sigma^{34,35}$ , where  $\langle r^{-3} \rangle_{2p}$  is the expectation value of  $r^{-3}$  for the  $2p_z$  orbital of the central carbon site, and  $\sigma$  is the fractional spin density in the molecular orbital.

These simple arguments assuming uniaxial angular dependences of the chemical shift and the Knight (spin) shift bring about the shifts with the same principal axis, but with the opposite signs. In the real material, however, the compensation between these two effects is not complete since the chemical shift has non-uniaxial symmetry.

## B. Line splitting of the spectra

The two  $^{13}\text{C}$  sites in the TMTTF molecule are crystallographically inequivalent in the crystal, which are the inner and the outer carbons from the inversion center. When external magnetic field is applied along the magic angle where doubly split lines due to the nuclear dipolar interaction overlaps, we obtain  $^{13}\text{C}$  NMR spectra as shown in Fig. 2 composed of two distinct lines, *A* and *B*, at 200 K. Each distinct line split into two peaks below 102 K, that is consistent with the reported data discussed to be the evidence for the charge ordering.<sup>30</sup> In Fig. 3, we plot the temperature dependences of the peak positions from the shift origin defined as the peak frequency at the lowest temperature. Each line above 102 K symmetrically splits at  $T_{\text{CO}}$ , so that the averaged frequency of the two (four) peaks of the spectra plotted as solid line is unchanged at this temperature. This shows that the total spin density is conserved at  $T_{\text{CO}}$ . The line splitting takes place between 102 K and 95 K. Below 95 K, four peaks are nearly independent of temperature.

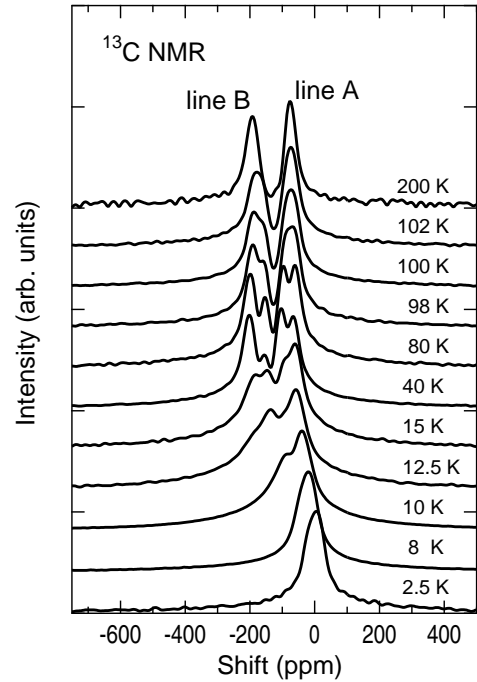


FIG. 2: The  $^{13}\text{C}$  NMR spectra at various temperatures. We label distinct lines as lines *A* and *B* from the peak at the highest frequency above 102 K, and as *A*<sub>1</sub>, *A*<sub>2</sub>, *B*<sub>1</sub>, and *B*<sub>2</sub> between 15 K and 102 K.

## C. Nuclear spin lattice relaxation in the paramagnetic state

The nuclear spin lattice relaxation rate,  $1/T_1$  for the distinct lines are shown in Fig. 4. The  $1/T_1$  for line

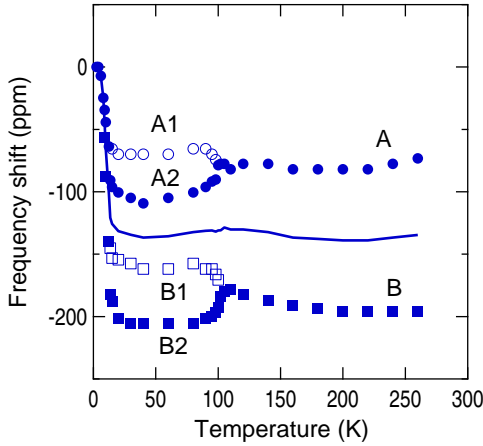


FIG. 3: The peak positions of the spectra. We define the peak position of the spectra at 2.5 K as the origin. The solid line is the averaged frequency of two (four) peak positions.

$A$  ( $1/T_1^A$ ) and that for line  $B$  ( $1/T_1^B$ ) both increase with temperature in a parallel manner above  $T_{\text{CO}}$  in a semilogarithmic scale. The  $1/T_1$  at site  $n$  is expressed as,  $1/T_1^n = \frac{2\gamma_n^2 T}{\mu_B^2} \sum_q {}^n F_{\perp}(q)^2 \chi''(q, \omega_L)/\omega_L$ , here  $\gamma_n$  is the gyromagnetic ratio of carbon,  ${}^n F_{\perp}(q)$  is the  $q$  dependent hyperfine coupling constant at site  $n$ ,  $\chi''$  is the imaginary part of the dynamic susceptibility, and  $\omega_L$  is the Larmor frequency. Thus, the only difference between  $1/T_1^A$  and  $1/T_1^B$  is ascribed to that of  ${}^n F_{\perp}(q)$ . Here  $F_{\perp}(q)$  is expected to have little  $q$  dependence in organic conductors, therefore exclusively depends on the spin density at the nucleus. Since  $1/T_1^A$  appears twice as large as  $1/T_1^B$  above  $T_{\text{CO}}$ , we conclude that line  $A$  ( $B$ ) in the frequency domain is due to the inner (outer) carbon site in the TMTTF molecule since the spin density on the inner carbon is estimated to be about 1.4 times as that on the outer one.<sup>21,36</sup>

Below  $T_{\text{CO}}$ , while  $1/T_1^{A1(B1)}$  (the  $1/T_1$  for the inner (outer) carbon in the charge donating molecules) monotonously decreases upon cooling,  $1/T_1^{A2(B2)}$  (that for the charge accepting molecules) first increase and then turn to decrease. This fact evidences that the line splitting of the NMR spectra at 102 K is at least originated from the difference of charge (spin) densities since the dominating source to the nuclear relaxation process here is expected to be the spin correlation function. It should be mentioned that the charge disproportionation takes place gradually from 102 K to about 60 K, although the line splitting occurs within a narrow temperature range of 5 K. This difference indicates that the contribution of the chemical shift to the frequency shift is larger than that of the spin shift at  $T_{\text{CO}}$ .

The previously reported  $1/T_1$  for the charge accepting sites ( $1/T_1^{A2(B2)}$  in this paper) is nearly independent of temperature between 80 K and 40 K argued to be due to low-dimensional “magnetic” correlations among spin

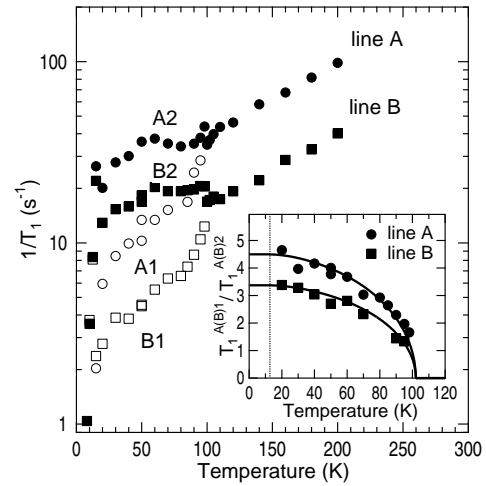


FIG. 4:  $1/T_1$  for distinct lines. The ratios  $T_1^{A1(B1)}/T_1^{A2(B2)}$  in the charge ordered state are plotted in the inset.

$1/2$ ’s realized by the charge ordering.<sup>31</sup> In the present study, however,  $1/T_1^{A2(B2)}$  decreases from 60 K to 20 K in a nearly parallel manner in a logarithmic scale to that for the charge donating sites.

We plot the ratio  $T_1^{A1(B1)}/T_1^{A2(B2)}$  in the inset of Fig. 4. The ratio shows rapid growth just below  $T_{\text{CO}}$  but finally saturates in approaching  $T_{\text{SP}}$ , showing the development of charge ordering. Therefore, we conclude that both the charge accepting and donating carbons follow one electron correlation function, and that the charge ordering discussed here seems to open a (pseudo) gap for the spin excitation spectra, which differ the  $1/T_1$  for the charge accepting and donating sites. Since the both charge accepting and donating sites follow the same correlation function, the ratio equals  $({}^{A(B)} F_{\perp}(q)/{}^{A(B)} F_{\perp}(q))^2$ . Assuming that  $F_{\perp}(q)$  exclusively proportional to the charge density, it is derived that the ratio of the charge densities is about 2:1.

#### IV. SPIN-PEIERL'S STATE

Here we focus on the electronic state in the vicinity and below the spin-Peierls phase transition, as summarized in Figs. 5 and 6. As shown in Fig. 5 (a), the strong cusp at 14 K for the averaged frequency (solid line) and the pronounced loss of spin density below this temperature shows the phase transition to the spin singlet ground state.

It is noteworthy that only two distinct lines are visible in the NMR spectra below  $T_{\text{SP}}$ . If the charge ordering have survived in the spin-Peierls state upon cooling, four lines would be observed with monotonous decrease of the interval frequency between the two lines originated from charge accepting and donating carbons.

In Fig. 5 (b), we plot the difference between each peak

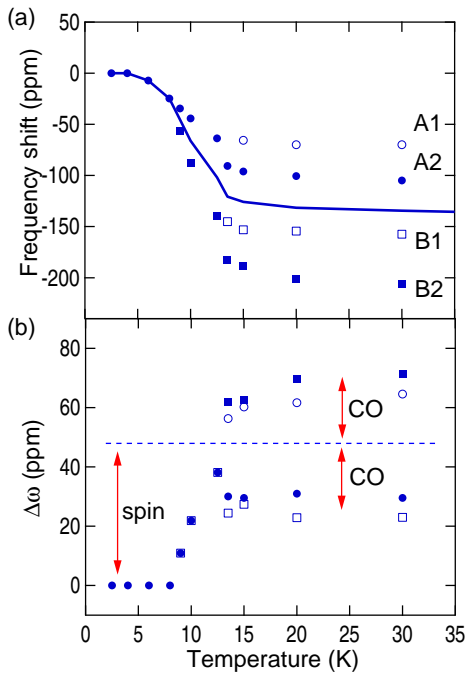


FIG. 5: (a) The peak positions in the vicinity and below  $T_{SP}$ . (b) The gaps between the peak positions and the averaged frequency denoted shown as the solid line in (a). The dashed line shows the spin contribution to  $\Delta\omega$ .

positions and the averaged frequency as the solid line in Fig. 5 (a), ( $\Delta\omega \equiv |\nu_{\text{res},i} - \frac{1}{4}\sum_{i=1}^4 \nu_{\text{res},i}|/\nu_0$ ). Here,  $\nu_{\text{res}}$  is the peak frequency of the spectra and  $\nu_0$  is the Larmor frequency. Even in the paramagnetic state, two  $\Delta\omega$  for the charge rich sites slightly decrease while two  $\Delta\omega$  for the charge poor sites increase from 20 K to 14 K. The fact that  $\Delta\omega$  at 12.5 K is about the averaged value of the four  $\Delta\omega$  at 14 K excludes the possibility that the merging of the distinct lines is originated from loss of the total spin density due to the spin-Peierls transition.

Likewise, the  $1/T_1$  at 12 K located in between those at 14 K as shown in Fig. 6 is consistent with the change in  $\Delta\omega$ . This suggests that two inequivalently charged molecules below  $T_{CO}$  again merge at  $T_{SP}$ .  $1/T_1$  below  $T_{SP}$  well follows the activated temperature dependence ( $1/T_1 \propto \exp(-\Delta/T)$ ) as shown in Fig. 6, and yields  $\Delta=43$  K as the activation energy.

In addition to the spin contribution to our observations, the chemical shift that is originated from the motion of electrons on the molecular orbitals is reported to be affected by charge ordering.<sup>20</sup> The lowest temperature  $^{13}\text{C}$  NMR spectra for  $\theta$ -(BEDT-TTF)<sub>2</sub>RbZn(SCN)<sub>4</sub> that has spin-singlet ground state have two distinct peaks with the splitting of 80 ppm. Since the chemical shift is expected to be unchanged against the spin-Peierls transition, the only source of the line splitting is the differentiation in the chemical shift caused by inequivalently charged molecules. Therefore, again, our observation of

only one peak in the NMR spectra at the lowest temperature indicates the absence or the strong suppression of the charge ordering in this material.

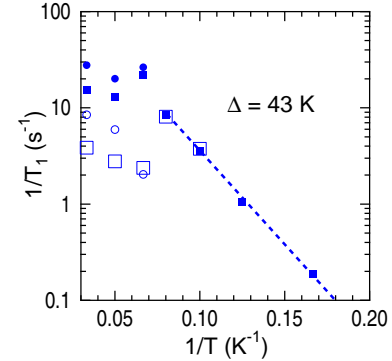


FIG. 6:  $1/T_1$  for the distinct lines below 30 K. The dashed line shows the activated temperature dependence with  $\Delta = 43$  K.

## V. DISCUSSION

We have confirmed charge ordering by the doubly split NMR spectra and corresponding differentiation in  $1/T_1$  as shown in Sec. III below 102 K. This is consistent with the previously reported results of  $^{13}\text{C}$  NMR on this material above 30 K.<sup>31</sup> Reference 31 argues a possible scenario that spin-singlet correlation among spins only on the charge accepting molecules leads to the spin-Peierls transition based on their results of  $1/T_1$  that becomes independent of temperature between 40 K to 80 K, indicating one dimensional “magnetic” correlations. This argument naturally leads to a coexistence of charge ordered and spin-Peierls states that is theoretically reproduced based on a one-dimensional Hubbard model with lattice distortions.<sup>37</sup>

Theoretically, it is widely considered that the Coulomb repulsion among the electrons stabilizes the charge ordered state in a quarter-filled Q1D electronic system. In particular, the interplay between charge ordering and lattice instability can realize various patterns of charge ordering.<sup>10,11,12,13,14,15,16,17,18</sup> The stable charge configurations are CDW or BOW (bond-order wave) with  $4k_F$  (or  $2k_F$ ) periodicity including their coexistences. Of these, it is pointed out that the charge modulations of which antinodes are located in between two molecular sites such as BOW or BCDW (CDW with bond ordering) do not require significant charge disproportionation on the molecules.<sup>12,15,16,17</sup>

The coexisted electronic state of  $4k_F$  CDW and spin-Peierls, theoretically realizable, is indeed one possible scenario that resolve two phase transitions of this material.<sup>37</sup> This argument can include one-dimensional mag-

netic correlation among spin 1/2 realized at the charge accepting molecules. On the other hand, charge ordering is not a necessary condition for spin-Peierls instability as indicated by DCNQI based organic conductor which is other example of Q1D quarter-filled system. In this system, although  $(\text{DI-DCNQI})_2\text{Ag}$  which undergoes antiferromagnetic state shows charge ordering transition well above  $T_N$ ,  $(\text{DMe-DCNQI})_2\text{Ag}$  which undergoes spin-Peierls transition shows no charge ordering.<sup>19</sup> The antiferromagnetic correlation which has  $2k_F$  periodicity is considered to be that among the spin 1/2 realized by dimerized molecules without charge ordering (“dimer Mott insulator”).<sup>38,39</sup> As the charge configuration or the spin correlation, this “dimer Mott” type mechanism toward the spin-Peierls state can not be excluded.

In the present study that covers the temperature range across the spin-Peierls transition, the merging of the split spectra shown in Sec. III B reveals a disappearance or a strong suppression of the charge ordering below  $T_{\text{SP}}$ . These observations seems to exclude the simple scenario that the development of spin singlet correlation among spin 1/2’s that are located at the molecular positions provokes the spin-Peierls transition. In other words, the spin-Peierls transition predominantly induces bond ordering with  $2k_F$  periodicity or reduces site ordering. Moreover, both  $1/T_1$  for the charge accepting and donating molecules decrease in a parallel manner in approaching  $T_{\text{SP}}$ , indicating only one spin correlation function even in the charge ordered state. This finding indicates considerable interaction between the charge accepting and donating sites, and is consistent with bond ordered spin-Peierls state.

As the origin of the redistribution of charge densities at  $T_{\text{SP}}$ , we can cite two possibilities which focus on electronic origin only and the coupling between the electronic correlation and lattice degree of freedom. One is a competitive interplay between two patterns for the charge ordering which would suppress the charge ordering. In contrast to the  $4k_F$  periodicity which is stabilized by Coulomb repulsions, the spin-Peierls state has  $2k_F$  modulation. The tetramization of the molecules can vary the charge configuration, and particularly induce charge transfers between two dimerized molecules. In addition to the electronic origin, the variation in the lattice parameters due to the spin-Peierls transition vary the charge transfers or Coulomb repulsion, that can reduce on-site type (CDW type) charge ordering. Indeed, it is reported that the charge ordering in this material is so fragile that charge ordered paramagnetic state vanishes at a pressure as low as 0.15 GPa, indicating considerable effect of lattice degree of freedom against the electronic correlations.<sup>31</sup>

## VI. CONCLUSION

We demonstrate the frequency shifts and  $1/T_1$  of central  $^{13}\text{C}$  sites for the quarter-filled Q1D material

$(\text{TMTTF})_2\text{AsF}_6$  from the room temperature to 2 K. The split of the distinct lines of the NMR spectra and the appearance of two  $1/T_1$  which show different temperature dependences below 102 K evidence the charge ordering. The ratio of two  $1/T_1$  for the charge accepting and donating sites which grows from  $T_{\text{CO}}$  in lowering temperature and finally saturates in approaching  $T_{\text{SP}}$  suggests the development of charge ordering. This shows that there exists only one spin correlation function even in the charge ordered state and the ratio of charge ordering is 2:1. Moreover it is also indicated that the nuclear relaxation process feels a kind of gap which realizes the different  $1/T_1$  originated from the charge ordering.

In the vicinity or below the spin-Peierls transition, however, the split lines of the NMR spectra again merge by a charge origin. This shows a strong suppression of the charge ordering or a redistribuion of ordered charge densities at the spin-Peierls transition.

## Acknowledgments

One of the authors (S. F.) is grateful to K. Yonemitsu, H. Seo and K. Kanoda for fruitful discussions. This work is supported by a Grant-in-Aid for Scientific Research on Priority Area, “Novel Functions of Molecular Conductors under Extreme Conditions” from the Ministry of Education, Culture, Sports, Science and Technology, and by a Grant-in-Aid for Scientific Research (No. 13640375) from Japan Society for the Promotion of Science.

## APPENDIX: ANGULAR DEPENDENCE OF THE SPECTRA ALONG THE $a$ - $b$ PLANE

As we discuss in Sec. III A, the frequency shift is reduced because the chemical shift and the spin shift have opposite signs when the external fields are rotated in the  $b$ - $c$  plane. Therefore, this experimental condition prevent a precise estimation of the hyperfine coupling tensor for  $^{13}\text{C}$  in TMTTF CTS.

In this Appendix, we demonstrate the orientation dependence of the frequency shifts where the field direction is rotated from  $H \parallel a$  to  $H \parallel b$ . In approaching the  $a$ -axis (molecular stacking axis), the spin contribution to the frequency shift is expected to be larger because the external fields becomes closer to perpendicular to the molecular plane.

We plot the peak positions of the NMR spectra in Fig. 7. At 5 K, two lines are observed with a parallel gap along the rotation axis, which is due to the constant angle between the magnetic field and C-C doubled bond in the TMTTF molecule. The only source for the angular dependence is that of the chemical shift. At 240 K, we plot only two peaks that locate at the highest and lowest frequencies. Remaining two peaks are stemmed from the nuclear dipolar interaction, which show parallel curves with two solid lines. At 50 K in the charge ordered state,

we also plot two peaks in the highly complicated spectra. Here, 8 peaks are visible at most, that is consistent with the charge ordering as shown in Sec. III B.

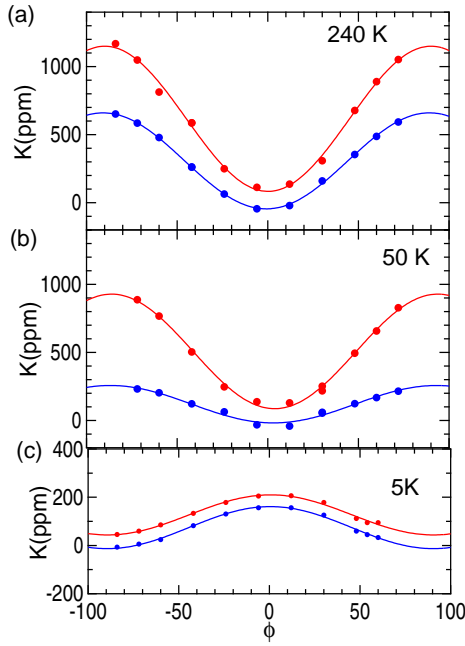


FIG. 7: Angular dependence of the frequency shifts along the *a*-*b* plane at (a) 240 K, (b) 50 K, and (c) 5 K. At 240 (50) K, we plot only two peak positions although 4 (8) lines are observed. See the text.

We summarize in Table I the fitted parameters of the

peak positions in Fig. 7 to the uniaxial function  $\nu_{\text{obs}} = \sigma_{\text{iso}} + \sigma_{\text{ax}}(1 - 3 \cos^2 \phi) + K_{\text{iso}} + K_{\text{ax}}(1 - 3 \cos^2 \phi)$ . Here  $\nu_{\text{obs}}$  is the observed frequency,  $\sigma_{\text{iso}}(\sigma_{\text{ax}})$  is the isotropic (anisotropic) part of the chemical shift, and  $K_{\text{iso}}(K_{\text{ax}})$  is the isotropic (anisotropic) part of the Knight shift, respectively. We defined the shift origin as the isotropic part of the chemical shift.

TABLE I: Fitted parameters for the angular dependence of the peak frequencies of the NMR spectra for Fig. 7. The shift origin is defined by the isotropic component of the chemical shift. The unit is ppm.

	isotropic	anisotropic
$\sigma$	0	-56.7
$K_{\text{s}}^1$	68.8	302.5
$K_{\text{s}}^2$	284.2	410.2

The obtained spin contributions to the frequency shifts are more than 3 times as large as those in the *b*-*c* plane, therefore we can estimate the ratio of the charge densities in the charge ordered state by the splitting of the NMR spectra. Since we can consider that the ratio of the spin densities for outer and inner carbons in the same molecule is unchanged across the charge ordering, the spectra at 50 K as shown in Fig. 7 locates between the outer carbon in the charge donating molecule and inner carbon in the charge accepting molecule. By comparing the angular dependence of the spectra at 50 K and 240 K, we obtain the ratio as  $(K_{\text{ax}}^1/K_{\text{ax}}^2(50\text{K}))/((K_{\text{ax}}^1/K_{\text{ax}}^2(240\text{K})) = 2.2$ . This value is consistent with the estimation by  $1/T_1$  in Sec. III C.

\* Present address: Department of Applied Physics, University of Tokyo, Hongo, Bunkyo-ku, Tokyo 113-8656, Japan, and CREST, Japan Science and Technology Corporation, Kawaguchi 332-0012, Japan; Electronic address: fujiyama@ap.t.u-tokyo.ac.jp

<sup>1</sup> J. Tranquada, B. Sternlieb, J. Axe, Y. Nakamura, and S. Uchida, *Nature (London)* **375**, 561 (1995).

<sup>2</sup> S. Mori, C.H. Chen, and S.W. Cheong, *Nature (London)* **392**, 473 (1998).

<sup>3</sup> T. Hanaguri, C. Lupien, Y. Kohsaka, D.-H. Lee, M. Azuma, M. Takano, H. Takagi, and J.C. Davis, *Nature (London)* **430**, 1001 (2004).

<sup>4</sup> H. Seo, C. Hotta, and H. Fukuyama, *Chem. Rev.* **104**, 5005 (2004).

<sup>5</sup> F. Nad, P. Monceau, and J.M. Fabre, *Eur. Phys. J. B* **3**, 301 (1998), F. Nad, P. Monceau, C. Carcel, and J.M. Fabre, *Phys. Rev. B* **62**, 1753 (2000).

<sup>6</sup> J.P. Pouget and S. Ravy, *Synth. Met.* **85**, 1523 (1997).

<sup>7</sup> Y. Nogami and T. Nakamura, *J. Phys. IV France*, **12**, Pr9-145 (2002).

<sup>8</sup> K. Yamamoto, K. Yakushi, K. Miyagawa, K. Kanoda, and A. Kawamoto, *Phys. Rev. B* **65**, 085110 (2002).

<sup>9</sup> K. Suzuki, K. Yamamoto, and K. Yakushi, *Phys. Rev. B* **62**, 7679 (2000).

**69**, 085114 (2004).

<sup>10</sup> J.E. Hirsch and D.J. Scalapino, *Phys. Rev. Lett.* **50**, 1168 (1983), *Phys. Rev. B* **29**, 5554 (1984).

<sup>11</sup> K. Penc and F. Mila, *Phys. Rev. B* **49**, 9670 (1994); **50**, 11429 (1994).

<sup>12</sup> J. Riera and D. Poilblanc, *Phys. Rev. B* **62**, 16243 (2000).

<sup>13</sup> H. Seo and H. Fukuyama, *J. Phys. Soc. Jpn.* **66**, 1249 (1997).

<sup>14</sup> N. Kobayashi and M. Ogata, *J. Phys. Soc. Jpn.* **66**, 3356 (1997), N. Kobayashi, M. Ogata, and K. Yonemitsu, *ibid.* **67**, 1098 (1998).

<sup>15</sup> K.C. Ung, S. Mazumdar, and D. Toussaint, *Phys. Rev. Lett.* **73**, 2603 (1994).

<sup>16</sup> S. Mazumdar and S. Ramasesha, *Phys. Rev. Lett.* **82**, 1522 (1999).

<sup>17</sup> R.T. Clay, S. Mazumdar, and D.K. Campbell, *Phys. Rev. B* **67**, 115121 (2003).

<sup>18</sup> S. Mazumdar, R.T. Clay, and D.K. Campbell, *Phys. Rev. B* **62**, 13400 (2000).

<sup>19</sup> K. Hiraki and K. Kanoda, *Phys. Rev. Lett.* **82**, 2412 (1998).

<sup>20</sup> K. Miyagawa, A. Kawamoto, and K. Kanoda, *Phys. Rev. B* **62**, 7679 (2000).

<sup>21</sup> As a review, *Organic Superconductors*, 2nd ed. ed. by T. Ishiguro, K. Yamaji, and G. Saito, Springer-Verlag, Heidelberg (1998).

<sup>22</sup> D. Jérôme, *Science*, **252**, 1509 (1991).

<sup>23</sup> H.J. Schultz, in *Strongly Correlated Electronic Materials* ed. by K.S. Bedell *et al.* Addison-Wesley, Reading, MA (1994).

<sup>24</sup> J-I. Kishine and K. Yonemitsu, *Int. J. Mod. Phys. B* **16**, 711-771 (2002).

<sup>25</sup> T. Nakamura, R. Kinami, T. Takahashi, and G. Saito, *Synth. Met.* **86**, 2053 (1997).

<sup>26</sup> T. Nakamura, T. Nobutoki, Y. Kobayashi, T. Takahashi, and G. Saito, *Synth. Met.* **70**, 1293 (1995).

<sup>27</sup> S. Fujiyama and T. Nakamura, *Phys. Rev. B* **70**, 045102 (2004).

<sup>28</sup> P. Delhaes, C. Coulon, J. Amiell, S. Flandrois, E. Toreilles, J.M. Fabre, and L. Giral, *Mol. Cryst. Liq. Cryst.* **50**, 43 (1979).

<sup>29</sup> R. Laversanne, C. Coulon, B. Gallois, J.P. Pouget, and R. Moret, *J. Physique Lett.* **45**, L393 (1984).

<sup>30</sup> D.S. Chow, F. Zamborszky, B. Alavi, D.J. Tantill, A. Baur, C.A. Merlic, and S.E. Brown, *Phys. Rev. Lett.* **85**, 1698 (2000).

<sup>31</sup> F. Zamborszky, W. Yu, W. Raas, S.E. Brown, B. Alavi, C.A. Merlic, and A. Baur, *Phys. Rev. B* **66**, 081103 (2002).

<sup>32</sup> S.M. De Soto, C.P. Slichter, A.M. Kini, H.H. Wang, U. Geiser, and J.M. Williams, *Phys. Rev. B* **52**, 10364 (1995).

<sup>33</sup> This argument is consistent with the common feature of the chemical shift. e.g. M. Mehring, *Principles of High Resolution NMR in Solids*, Springer-Verlag, Berlin, Heidelberg (1976).

<sup>34</sup> A. Abragam and M.H. Pryce, *Proc. Roy. Soc. A* **205**, 135 (1961).

<sup>35</sup> J. Owen and J.H.M. Thornley, *Rep. Prog. Phys.* **29**, 675 (1966).

<sup>36</sup> N. Kinoshita, M. Tokumoto, H. Anzai, T. Ishiguro, G. Saito, T. Yamabe, and H. Teramae, *J. Phys. Soc. Jpn.* **53**, 1504 (1984).

<sup>37</sup> M. Kuwabara, H. Seo, and M. Ogata, *J. Phys. Soc. Jpn.* **72**, 225 (2003).

<sup>38</sup> K. Yonemitsu and J-I. Kishine, *J. Phys. Chem. Solids* **62**, 99 (2001).

<sup>39</sup> K. Yonemitsu, *Phys. Rev. B* **56**, 7262 (1997).